C.P. No. 778

MINISTRY OF AVIATION

AERONAUTICAL RESEARCH COUNCIL

CURRENT PAPERS

Wind Tunnel Tests between M = 0.4 and 2.0 on a Cambered Wing of Slender Ogee Planform

by

M. D. Dobson and R. King-Underwood

LONDON: HER MAJESTY'S STATIONERY OFFICE

1965

SIX SHILLINGS NET

U.D.C. No. 533.693.4 : 533.6.043.1

C.P. No. 778

December 1963

WIND TUNNEL TESTS BETWEEN M = 0.4 AND 2.0 ON A CAMBERED WING OF SLENDER OGEE PLANFORM

by

M. D. Dobson
and
R. King-Underwood

SUMMARY

Results are presented of wind tunnel tests made to examine the lift, longitudinal stability and drag of a cambered wing with an ogee planform in the Mach number range 0.40 to 2.00. Some flow visualisation tests have also been made and photographs of the patterns obtained are included.

Replaces R.A.E. Tech. Note No. Aero 2933 - A.R.C. 25 837.

CONTENTS

ILLUSTRATIONS

ILLUSTRATIONS (Contd)

1 INTRODUCTION

As part of the research programme on wing design for a supersonic transport aircraft, tests were made in the 3 ft wind tunnel on a series of slender wings, some of which were plane and some of which had varying amounts of camber. The programme was intended to investigate the principal aerodynamic characteristics of the models and to examine the flow patterns which existed.

Measurements of normal force, pitching moment and axial force were made over the Mach number range 0.40 to 2.00 on one such cambered model, of ogee planform, which represented a possible aircraft shape. Surface flow patterns were examined by means of the oil-flow technique. The lateral stability characteristics of this model are being reported separately[1].

2 EXPERIMENTAL DETAILS

2.1 Model

The wing design was based on slender wing theory following the general design principles outlined by Maskell and Weber in Ref.2. The wing thickness distribution resembled that of a possible aircraft. The camber surface which has a design C_L of 0.025 was chosen so that the centre of pressure at this C_L was at 0.585 C_o. This centre of pressure position, which was 0.12 C_o ahead of the slender wing aerodynamic centre, was chosen to give (assuming linear development with C_L) a centre of pressure 0.04 C_o ahead of the aerodynamic centre at the cruise C_L, ($\simeq$ 0.075). Weber's camber design method[3] gives a family of camber surfaces with this design condition; the surface finally arrived at was a compromise between various requirements outlined in Ref.2, together with a limit of leading-edge droop, particularly near the wing apex since previous tests have shown that large leading-edge droops can adversely affect the vortex development and so, possibly lead to a severe loss of lift.

Fig.1 is an outline drawing of the model showing clearly the ogee planform; the inset curve shows the variation of the leading-edge sweepback angle along the leading-edge. Fig.2 illustrates the extent of the camber by showing cross sections through the model at various stations on C_o and the curve at the top of the figure shows how the various cross sections are displaced relative to each other by the chordwise camber. Fig.3 contains the main details of the model together with the equations of the leading-edge and the spanwise camber shoulder line.

The model was an aluminium-bronze casting of such quality of surface finish that little hand finishing was required and apart from coatings of black cellulose paint the model was virtually ready for the tunnel direct from casting. This method of manufacture gave a quick useful model but by supersonic wind tunnel standards the accuracy of manufacture was very low. Generally the thickness of the model was within about 0.020 in. of the design value but locally (particularly near the apex) it was rather worse than this. The average thickness of the wing trailing edge was 0.038 in.; the manufacturing design value being 0.020 in.

In order to accommodate the sting support a cylindrical fairing was included on the model: this is shown in Fig.1.

2.2 Test details

The tests were made over a Mach number range of 0.40 to 1.02 in the slotted transonic working section[4] of the 3 ft tunnel and over a Mach number range of 1.42 to 2.00 in the supersonic section[5]. Tests were not made at Mach numbers above 1.02 in the transonic section because of the uncertainty of the effects of shock waves reflected from the tunnel walls. The model was tested through a nominal incidence range of -2° to 12°. The Reynolds number per inch was 0.13×10^6 at all Mach numbers except M = 2.00, where, owing to power limitations, it was reduced to 0.11×10^6.

Bands of distributed roughness were used to ensure that the boundary layer on the model was turbulent. They consisted of a mixture of carborundum grains and a suitable adhesive, applied so that closely spaced individual grains projected from a very thin layer of the adhesive. For the supersonic tests, grains of maximum height 0.007 in. with araldite adhesive were used and for the tests in the transonic section, grains of maximum height 0.0045 in. with aluminium paint adhesive. The distributed roughness was applied in a band about $\frac{3}{8}$ in. wide, normal to the leading-edge, beginning $\frac{1}{8}$ in. from it. No check was made of the effectiveness of the roughness in causing transition but it was thought to be satisfactory except at a Mach number of 2.00 at low lift. Any results which are doubtful because of a suspected failure of the roughness to cause transition are indicated in the text.

The tests consisted of measurements of normal force, pitching moment and axial force using a strain-gauge balance incorporated in the sting support. Base pressure was measured by a pressure tube situated in the balance cavity. Flow visualisation tests were made using the surface oil-flow technique[6].

2.3 Accuracy of results

No interference corrections have been made to the transonic results obtained in the slotted working section as these are small but not accurately known. No corrections for flow asymmetry and curvature have been applied to results obtained in the supersonic working section as these are also small. The results have been corrected for sting deflections and balance interactions and the drag results have been corrected to a base pressure equal to free stream static pressure. The base area used in this correction did not include the area of the wing trailing-edge. No corrections have been made to account for the sting shield.

Forces and moments have been reduced to coefficient form with a moment reference point at 0.585 centre-line chord (C_o). The model constants used in computation of the coefficients were the wing projected area and the centre line chord length.

The results are estimated to be accurate to within the following limits:-

$M \pm 0.005$	$C_L \pm 0.005$
$\alpha \pm 0.05$	$C_m \pm 0.001$
	$C_D \pm 0.0005$

3 RESULTS

3.1 General

The tunnel data are tabulated in Table 1. In sections 3.2 to 3.5 the principal aerodynamic characteristics are described and briefly discussed. No attempt is made to draw general conclusions.

3.2 Lift

The lift curves, Fig.4, show non-linear tendencies which are similar at all test Mach numbers, though becoming less pronounced as Mach number is increased above M = 1.0. The lift curve for a given Mach number has a minimum slope at some positive C_L and the increase in slope away from this minimum is greatest at transonic speeds. The increases in lift curve slope are associated with leading-edge separations, which produce vortices above or below the wing according as the incidence is above or below the incidence for minimum slope. The fact that minimum slope occurs at a positive C_L results from the wing camber, which is intended to give attached flow at the design C_L (0.025). In this context it should be noted that the lift curve slopes show that this attachment condition occurs close to the theoretical design condition at M = 0.94 and M = 0.98 but rather above it at other Mach numbers. The variation of $\left(\frac{\partial C_L}{\partial \alpha}\right)_{MIN}$ with Mach number is shown in Fig.5.

3.3 Pitching moment

The pitching moment curves, Fig.6, have stable slopes throughout the test ranges but show non-linearities associated with the leading-edge separation. Fig.7 shows the variation of pitching moment coefficient with Mach number for C_L values of zero and 0.025 (design C_L).

The variation of aerodynamic centre position with Mach number for various values of C_L is shown in Fig.8. At low C_L ($C_L < 0.1$) the aerodynamic centre position is between 0.69 and 0.70 C_o at subsonic Mach numbers and between 0.74 and 0.75 C_o at supersonic Mach numbers, the rearward shift beginning at $M \simeq 0.90$. With increasing C_L the tendency is for the aerodynamic centre to shift forward at subsonic and supersonic Mach numbers and rearward between M = 0.90 and M = 1.02.

Curves showing the variation of centre of pressure position with C_L for each Mach number are plotted in Fig.9. Fig.10 shows the variation of centre of pressure position with Mach number for various values of C_L. At $C_L = 0.025$ the c.p. position lies between 0.58 and 0.59 C_o up to a Mach number of 0.86 above which it moves forward to 0.55 C_o at M = 0.98 and then aft to 0.585 C_o at M = 1.02. The supersonic c.p. position is 0.06 to 0.07 C_o aft of the subsonic position at $C_L = 0.05$ but rather less (0.05 C_o) at $C_L = 0.25$. It is interesting to note that at M = 1.0 and $C_L = 0.025$, the centre of pressure position is approximately 0.02 C_o ahead of the design position.

3.4 Drag

C_D versus C_L curves are shown in Fig.11 from which it will be seen that minimum drag for any Mach number does not occur at $C_L = 0$. This results from the asymmetric nature of the model due to the leading-edge camber. The value of C_L at which $C_{D_{MIN}}$ occurs varies with Mach number but is generally between 0.01 and 0.02. Curves showing the variation of C_{D_o} and $C_{D_{MIN}}$ with Mach number appear in Fig.12 and these show $C_{D_{MIN}}$ to be of the order 0.0005 less than C_{D_o} throughout the Mach number range. These curves are terminated at M = 1.82 as there is some doubt as to whether transition was taking place at the leading-edge at low C_L at M = 2.00. Values of C_{D_o} and $C_{D_{MIN}}$ at this Mach number therefore, are not to be trusted. C_D is plotted against C_L^2 in Fig.13 and above the value of C_L^2 for $C_{D_{MIN}}$ the curves are approximately linear. Since results for the same wing without camber are not available it is impossible to analyse the drag results in terms of the induced drag factor $K = \dfrac{\pi A\left(C_D - C'_{D_o}\right)}{C_L^2}$ where C'_{D_o} refers to the uncambered wing.

3.5 Flow development

The flow development was studied, by means of the surface oil flow technique, at Mach numbers of 0.40, 1.42 and 2.00. Figs.14, 15 and 16 indicate that the flow development with incidence at Mach numbers of 0.40, 1.42 and 2.00 is relatively straightforward. Up to about 5° incidence the flow remains attached over the upper surface but above this incidence signs of leading-edge separations are apparent over the outer parts of the wings. At incidences just above that at which separation first occurs there are signs of a number of distinct vortices, for example M = 0.4 at $\alpha = 6.1°$ and M = 1.42 at $\alpha = 6.8°$. However as incidence is further increased, these vortices combine in a single vortex on each side of the wing. This vortex then approaches the wing apex as incidence is increased.

It was suspected that at M = 2.0, at incidences below about 5°, transition of the boundary layer was not being fixed at the roughness band by the test grade of rou hness* (roughness A). Oil flow tests were therefore made at this Mach number at low incidences, firstly with a coarser grade of roughness (roughness B - maximum height 0.014 in.) and secondly with no roughness band. Roughness B fixed transition at the leading-edge under the test conditions and hence the flow photographs at $\alpha = 2.8^{\circ}$ and 4.8° in Fig.16 are of the model with this roughness. Fig.17 shows flow photographs of the case with no roughness at $\alpha = 2.8^{\circ}$ and for comparison the case with roughness A at this incidence. With transition free there appears to be separated flow at the leading-edge by $\alpha = 2.8^{\circ}$, and thus a very different flow pattern from the corresponding case with transition fixed is apparent.

SYMBOLS

A	aspect ratio
C_D	drag coefficient $\left(\frac{\text{drag}}{qS}\right)$
$C_{D_{MIN}}$	minimum drag coefficient
C_{D_o}	drag coefficient at zero lift
C_L	lift coefficient $\left(\frac{\text{lift}}{qS}\right)$
C_m	pitching moment coefficient $\left(\frac{\text{pitching moment}}{qS\ C_o}\right)$
C_o	centre line chord
c.p.	centre of pressure
$\frac{\partial C_L}{\partial \alpha}$	lift curve slope per radian
D	drag
h	distance of aerodynamic centre from apex
L	lift

---

*Past experience had indicated that roughness of this size was normally sufficient to fix transition under these test conditions.

SYMBOLS (Contd)

M	free stream Mach number
P	$\left[\frac{\text{wing area}}{\text{enclosing rectangle}}\right]$
q	kinetic pressure
S	wing area
S_T	semi span (at trailing-edge)
x	longitudinal displacement from apex (Fig.3)
x c.p.	distance of centre of pressure from apex
y	transverse displacement from centre-line (Fig.3)
z	vertical displacement from trailing-edge datum (Fig.2)
α	sting incidence plus corrections for bending under load
τ	$\left[\frac{\text{wing volume}}{\text{area}^{3/2}}\right]$

REFERENCES

No.	Author	Title, etc
1	McGregor, I.	Wind tunnel tests on the lateral stability of a cambered wing of slender ogee planform. Unpublished M.O.A. Report.
2	Maskell, E.C. Weber, J.	On the aerodynamic design of slender wings. J.R.Ae. Soc., Vol.63, No.588, pp.709 to 721. December 1959.
3	Weber, J.	Design of warped slender wings with the attachment line along the leading-edge. A.R.C. 20,051 September 1957.
4	Sutton, E.P. Caiger, M.T. Stanbrook, A.	Performance of the 36 x 35 inch slotted transonic working section of the R.A.E. Bedford 3 foot wind tunnel. A.R.C. R & M 3228 January 1960.

REFERENCES (Contd)

No.	Author	Title, etc
5	Morris, D.E.	Calibration of the flow in the working section of the 3 ft x 3 ft tunnel, National Aeronautical Establishment. A.R.C. C.P.261 September 1954.
6	Stanbrook, A.	The surface oil flow technique as used in high speed wind tunnels in the United Kingdom. R.A.E. Tech Note No. Aero 2712 A.R.C.22,385 August 1960.

TABLE 1

Table of results

M	α	C_L	C_m	C_D	M	α	C_L	C_m	C_D
0.40	-2.05	-0.080	0.0122	0.0138	0.90	-2.08	-0.091	0.0157	0.0140
	-1.02	-0.054	0.0093	0.0117		-1.04	-0.060	0.0115	0.0113
	0	-0.025	0.0058	0.0102		0.01	-0.029	0.0073	0.0097
	1.02	0.002	0.0026	0.0091		1.04	0	0.0035	0.0088
	2.04	0.025	0.0001	0.0092		2.08	0.024	0.0007	0.0088
	3.06	0.046	-0.0020	0.0097		3.12	0.049	-0.0023	0.0095
	4.08	0.068	-0.0042	0.0107		4.16	0.074	-0.0050	0.0108
	5.10	0.090	-0.0065	0.0121		5.21	0.101	-0.0083	0.0132
	6.13	0.121	-0.0099	0.0154		6.26	0.135	-0.0124	0.0171
	7.15	0.155	-0.0138	0.0198		7.31	0.172	-0.0174	0.0226
	8.18	0.188	-0.0174	0.0252		8.36	0.212	-0.0227	0.0306
	9.21	0.224	-0.0213	0.0331		9.42	0.251	-0.0277	0.0400
	10.25	0.259	-0.0243	0.0424		10.49	0.294	-0.0331	0.0521
	11.29	0.297	-0.0284	0.0542		11.55	0.337	-0.0387	0.0657
	12.32	0.334	-0.0316	0.0670		12.62	0.379	-0.0439	0.0810
0.70	-2.07	-0.085	0.0135	0.0141	0.94	-2.08	-0.094	0.0167	0.0147
	-1.04	-0.056	0.0100	0.0120		-1.04	-0.063	0.0122	0.0120
	0	-0.027	0.0064	0.0103		0.01	-0.031	0.0078	0.0100
	1.03	0.001	0.0029	0.0093		1.05	-0.001	0.0038	0.0088
	2.07	0.024	0.0003	0.0089		2.09	0.024	0.0008	0.0087
	3.10	0.047	-0.0021	0.0092		3.13	0.049	-0.0022	0.0093
	4.13	0.069	-0.0045	0.0104		4.17	0.074	-0.0050	0.0107
	5.17	0.096	-0.0073	0.0127		5.21	0.102	-0.0085	0.0133
	6.21	0.125	-0.0107	0.0160		6.26	0.137	-0.0129	0.0175
	7.25	0.161	-0.0151	0.0217		7.31	0.175	-0.0182	0.0238
	8.30	0.198	-0.0194	0.0282		8.37	0.216	-0.0240	0.0320
	9.35	0.234	-0.0233	0.0364		9.45	0.260	-0.0299	0.0466
	10.41	0.275	-0.0279	0.0473		10.54	0.301	-0.0355	0.0541
	11.47	0.312	-0.0317	0.0594					
	12.54	0.354	-0.0362	0.0743					

TABLE 1 (contd)

M	α	C_L	C_m	C_D	M	α	C_L	C_m	C_D
0.98	-2.07	-0.099	0.0187	0.0155	1.61	-2.05	-0.066	0.0126	0.0137
	-1.02	-0.066	0.0140	0.0126		-1.01	-0.037	0.0080	0.0112
	0.02	-0.033	0.0090	0.0105		0.02	-0.009	0.0035	0.0096
	1.05	-0.002	0.0045	0.0094		1.05	0.016	-0.0004	0.0090
	2.09	0.024	0.0011	0.0091		2.09	0.041	-0.0043	0.0092
	3.13	0.050	-0.0021	0.0097		3.12	0.064	-0.0080	0.0105
	4.18	0.075	-0.0049	0.0110		4.15	0.090	-0.0121	0.0127
	5.22	0.104	-0.0084	0.0135		5.19	0.116	-0.0161	0.0154
	6.27	0.141	-0.0136	0.0181		6.23	0.144	-0.0203	0.0197
	7.32	0.177	-0.0189	0.0242		7.27	0.176	-0.0254	0.0256
	8.37	0.225	-0.0269	0.0334		8.31	0.205	-0.0297	0.0327
	9.42	0.264	-0.0327	0.0433		9.36	0.237	-0.0343	0.0412
	10.47	0.311	-0.0406	0.0562		10.42	0.267	-0.0385	0.0507
	11.53	0.357	-0.0477	0.0711		11.47	0.297	-0.0425	0.0611
	12.59	0.402	-0.0546	0.0877		12.53	0.328	-0.0465	0.0732
1.02	-2.06	-0.099	0.0191	0.0173	1.82	-2.06	-0.066	0.0122	0.0133
	-1.03	-0.064	0.0132	0.0140		-1.02	-0.039	0.0080	0.0109
	0.01	-0.032	0.0086	0.0122		0.01	-0.014	0.0040	0.0094
	1.05	-0.001	0.0038	0.0111		1.04	0.011	0.0001	0.0087
	2.09	0.027	-0.0002	0.0111		2.07	0.034	-0.0035	0.0086
	3.13	0.055	-0.0041	0.0118		3.11	0.058	-0.0071	0.0094
	4.16	0.085	-0.0085	0.0136		4.15	0.082	-0.0108	0.0116
	5.20	0.116	-0.0133	0.0165		5.17	0.107	-0.0147	0.0146
	6.24	0.151	-0.0187	0.0211		6.21	0.133	-0.0186	0.0186
	7.29	0.191	-0.0252	0.0275		7.25	0.160	-0.0226	0.0238
	8.34	0.233	-0.0314	0.0361		8.29	0.188	-0.0267	0.0304
	9.39	0.277	-0.0383	0.0466		9.34	0.215	-0.0304	0.0380
	10.45	0.317	-0.0441	0.0583		10.39	0.244	-0.0342	0.0468
	11.51	0.363	-0.0511	0.0729		11.44	0.272	-0.0379	0.0567
	12.57	0.405	-0.0573	0.0888		12.50	0.299	-0.0413	0.0674
1.42	-2.04	-0.075	0.0153	0.0149	2.00	-2.05	-0.062	0.0112	0.0119
	-1.01	-0.045	0.0103	0.0123		-1.02	-0.036	0.0073	0.0092
	0.03	-0.016	0.0055	0.0106		0.01	-0.013	0.0039	0.0079
	1.06	0.011	0.0012	0.0098		1.03	0.011	-0.0003	0.0077
	2.09	0.036	-0.0028	0.0098		2.06	0.033	-0.0036	0.0078
	3.13	0.062	-0.0068	0.0111		3.08	0.055	-0.0069	0.0086
	4.16	0.088	-0.0108	0.0130		4.11	0.077	-0.0103	0.0102
	5.20	0.116	-0.0152	0.0158		5.14	0.101	-0.0139	0.0130
	6.24	0.146	-0.0200	0.0203		6.17	0.125	-0.0175	0.0168
	7.28	0.182	-0.0257	0.0266		7.20	0.151	-0.0212	0.0218
	8.33	0.216	-0.0309	0.0341		8.23	0.175	-0.0246	0.0296
	9.38	0.250	-0.0359	0.0434		9.27	0.201	-0.0281	0.0348
	10.43	0.285	-0.0411	0.0539		10.31	0.227	-0.0315	0.0428
	11.49	0.318	-0.0457	0.0654		11.35	0.253	-0.0348	0.0516
	12.55	0.352	-0.0504	0.0785		12.40	0.276	-0.0376	0.0617

Printed in England for Her Majesty's Stationery Office by the Royal Aircraft Establishment, Farnborough. W.P.60.K.4.

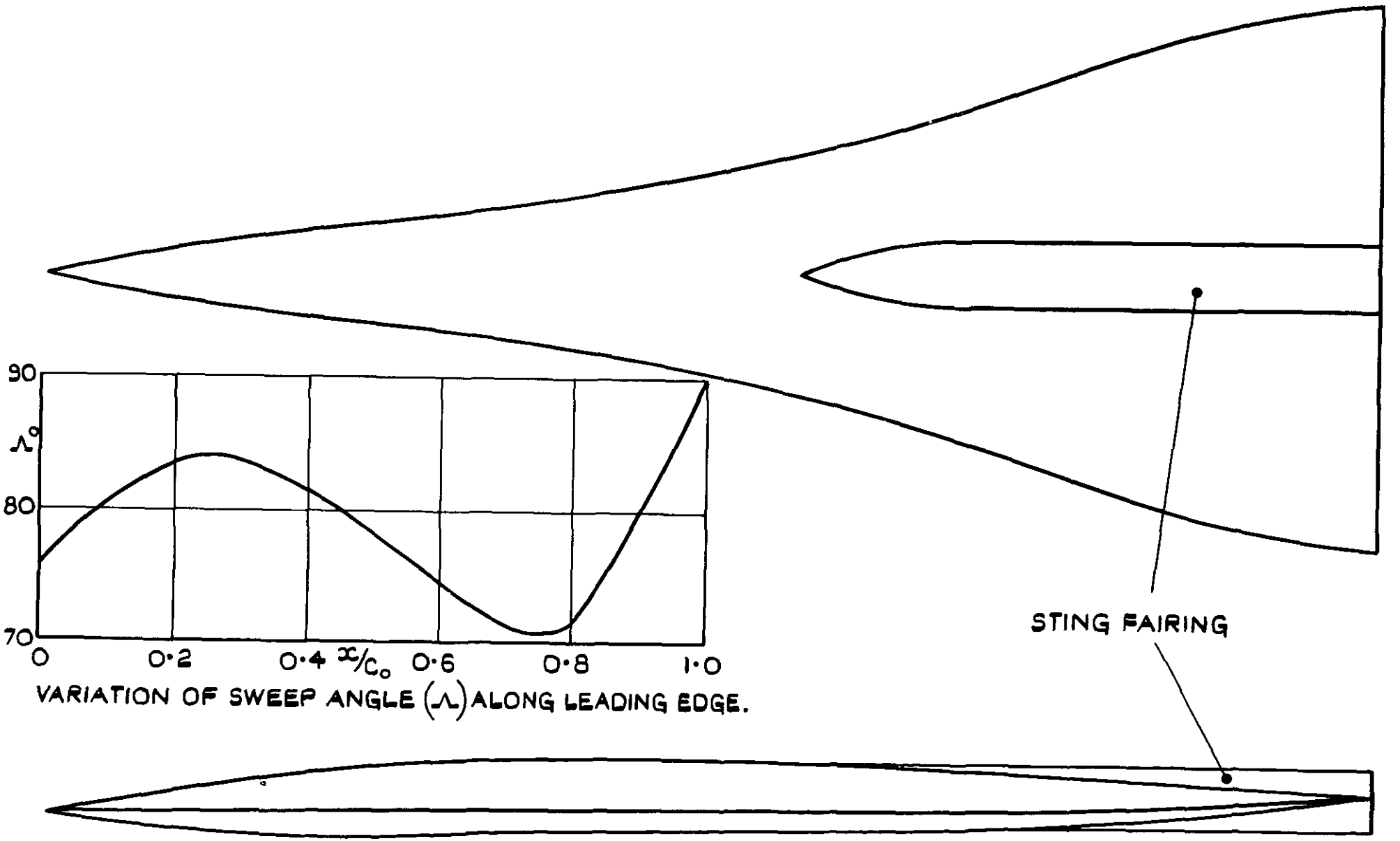

FIG. 1. OUTLINE DRAWING OF MODEL.

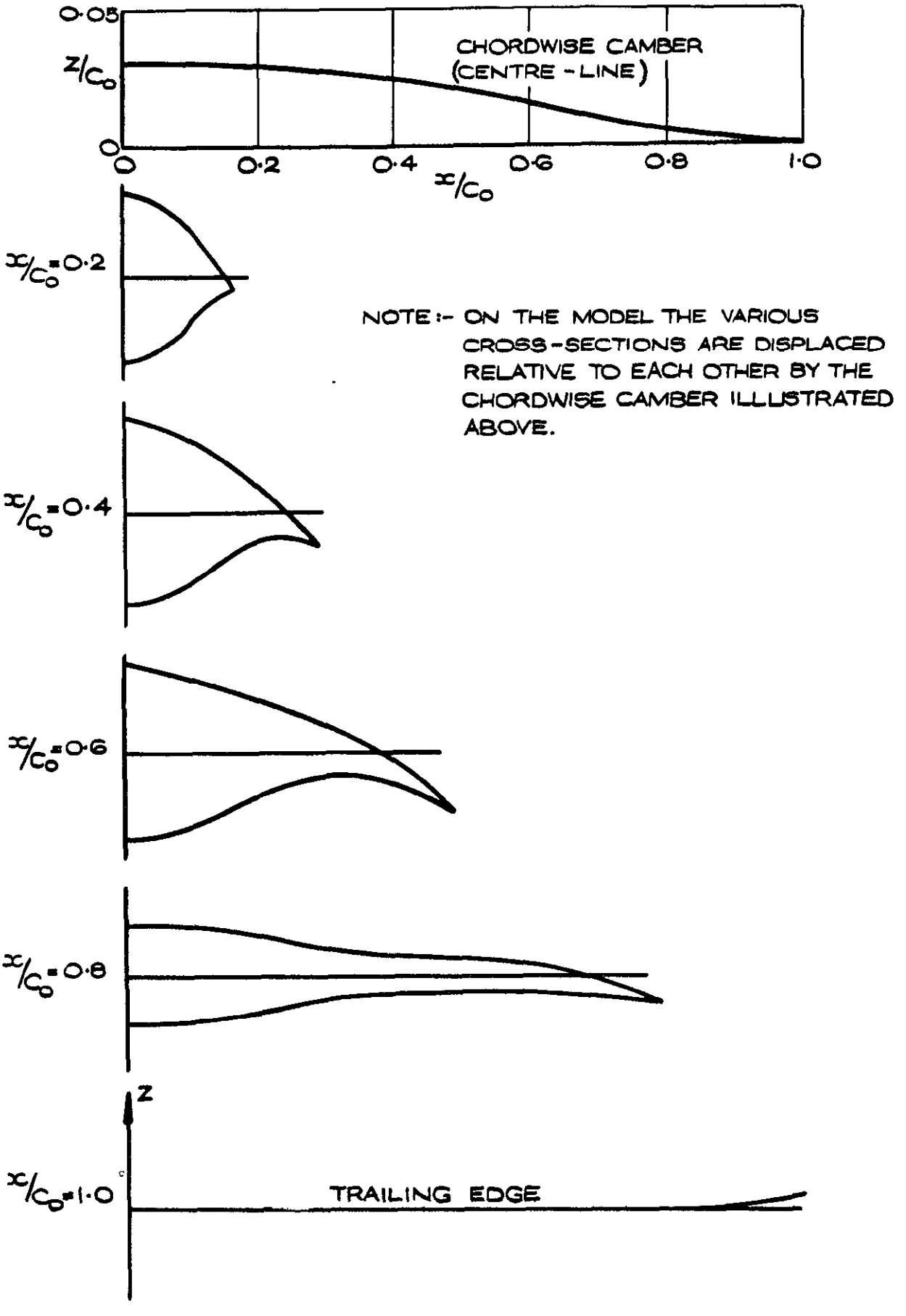

FIG. 2. SECTIONS THROUGH MODEL ILLUSTRATING CAMBER.

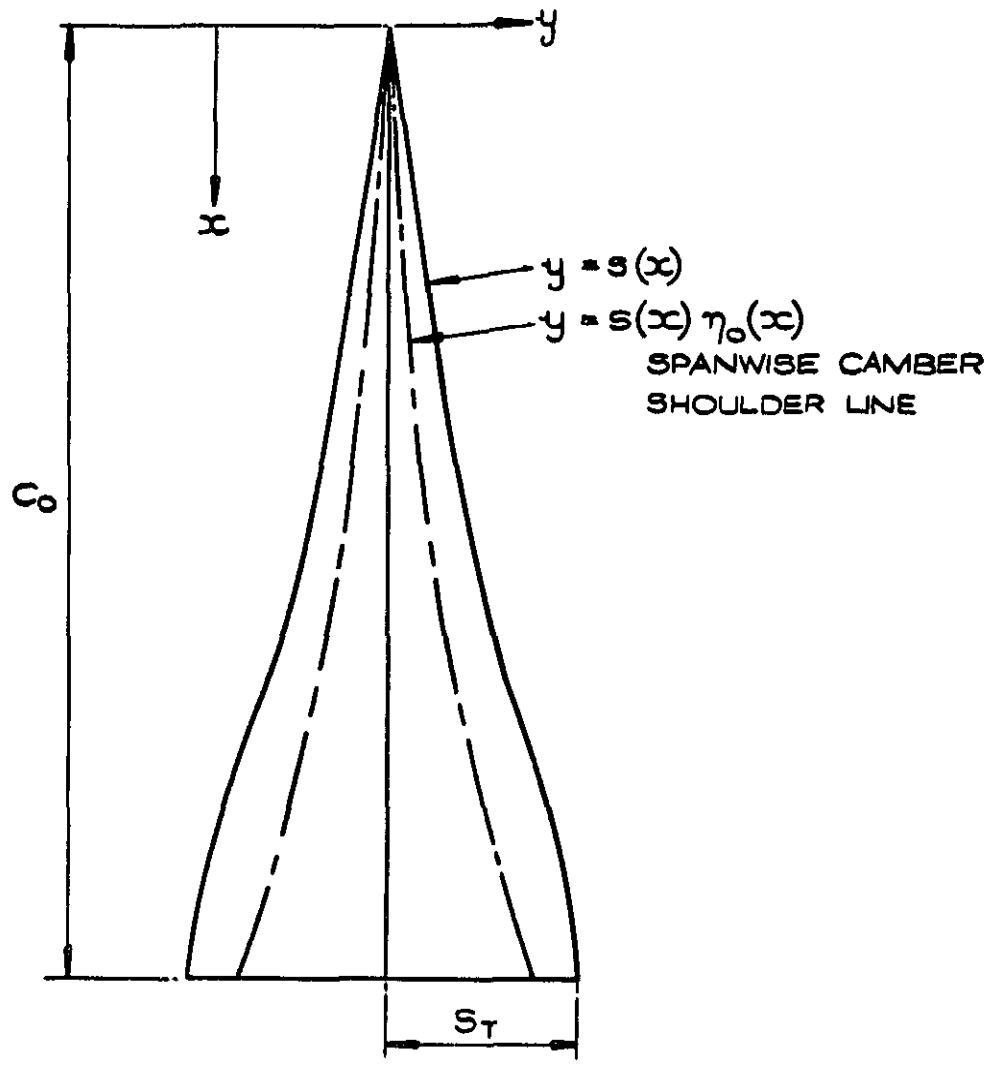

$s(x) = S_T x (1.2 - 2.4x + 2.2x^2 + 3x^3 - 3x^4)$

$\eta_0(x) = 0.5$ FOR $x \leq 0.5$

$= 0.5 + (x - 0.5)^2$ FOR $x > 0.5$

WING AREA = 135·1 SQ IN

WING CENTRE LINE CHORD (C_0) = 26·85 IN

WING SEMI SPAN (S_T) = 5·587 IN

$S_T/C_0 = 0.208$

$P \left(\frac{\text{WING AREA}}{\text{ENCLOSING RECTANGLE}}\right) = 0.45$

$\tau \left(\frac{\text{WING VOLUME}}{(\text{AREA})^{3/2}}\right) = 0.0415$

ASPECT RATIO (A) = 0·924

FIG.3. DETAILS OF WING.

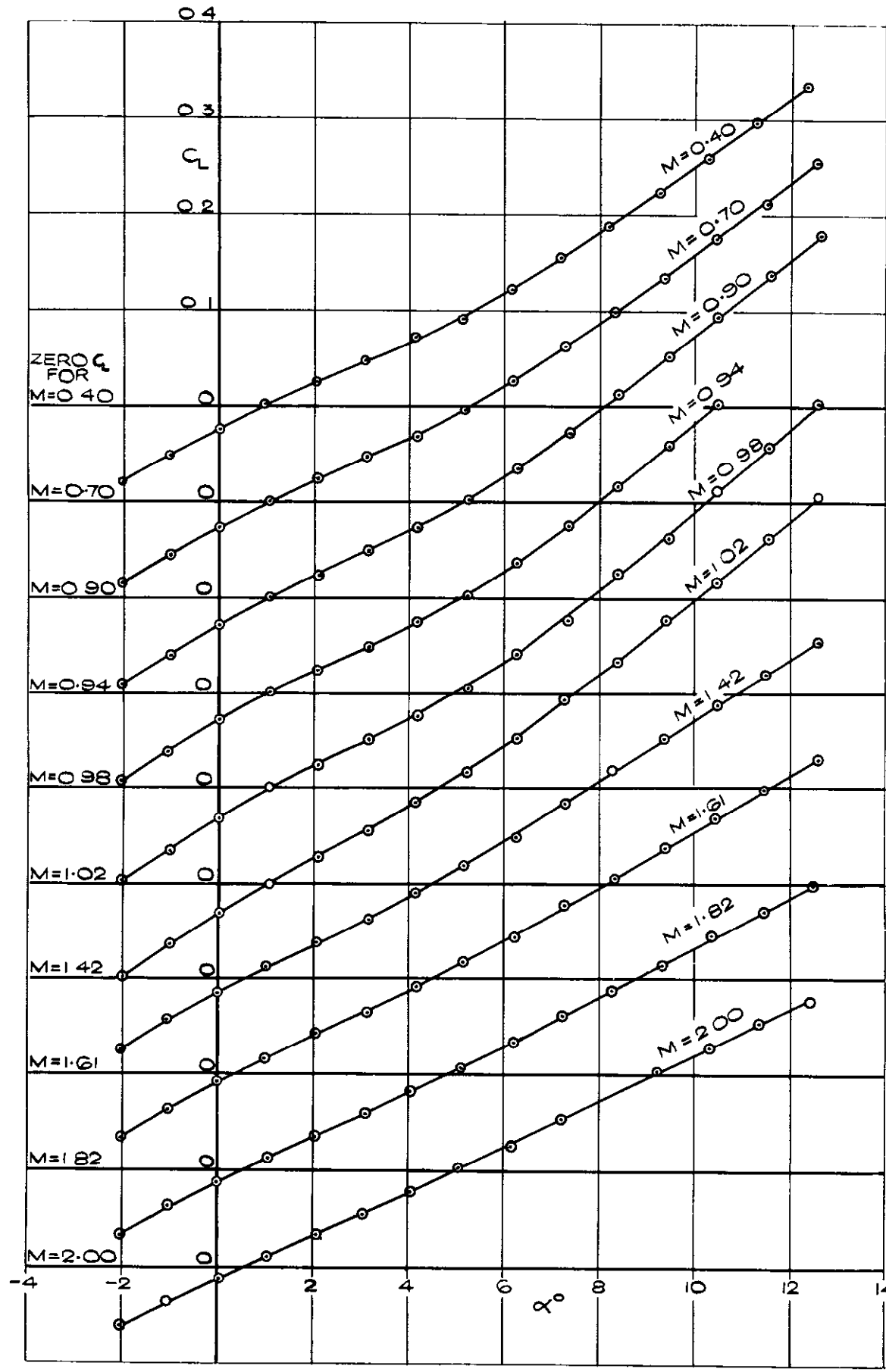

FIG. 4. VARIATION OF C_L WITH α.

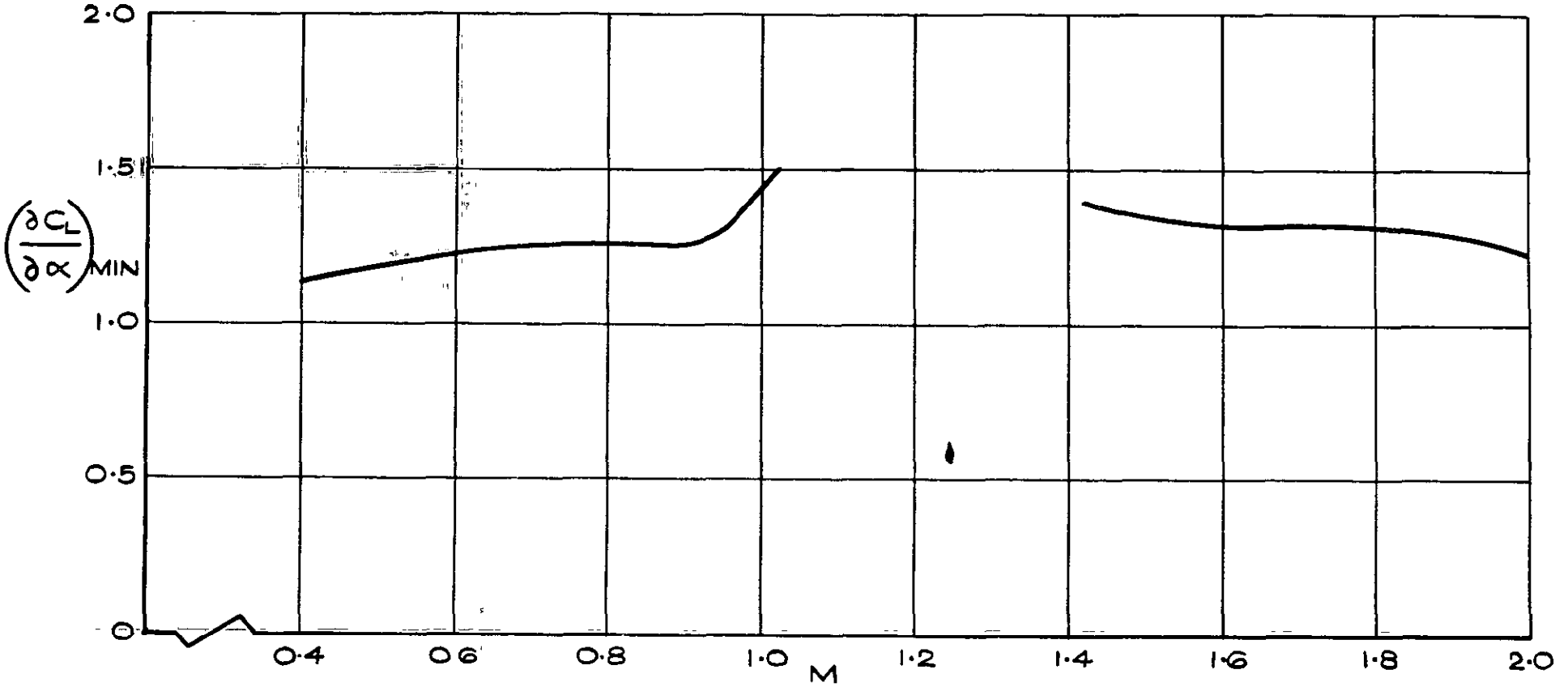

FIG.5. VARIATION OF $\left(\frac{\partial C_L}{\partial \alpha}\right)_{MIN}$ WITH MACH NUMBER.

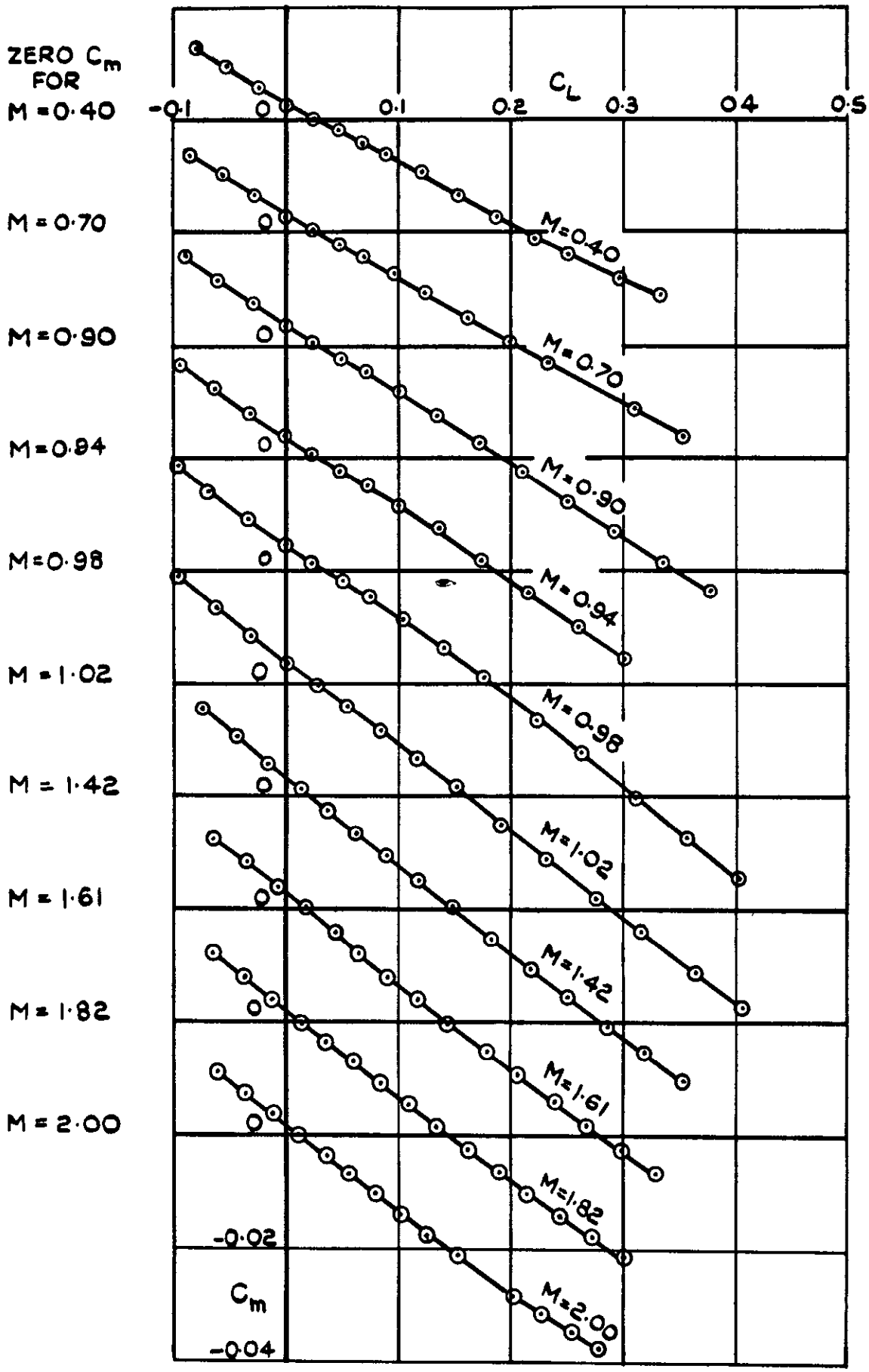

FIG. 6. VARIATION OF C_m WITH C_L.

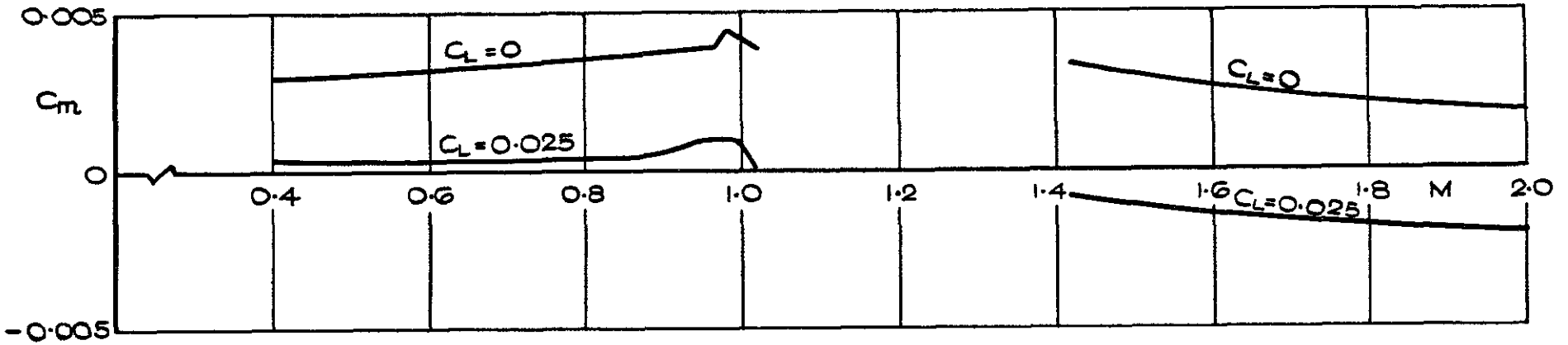

FIG.7. VARIATION OF C_m WITH M AT C_L VALUES OF 0 AND 0·025.

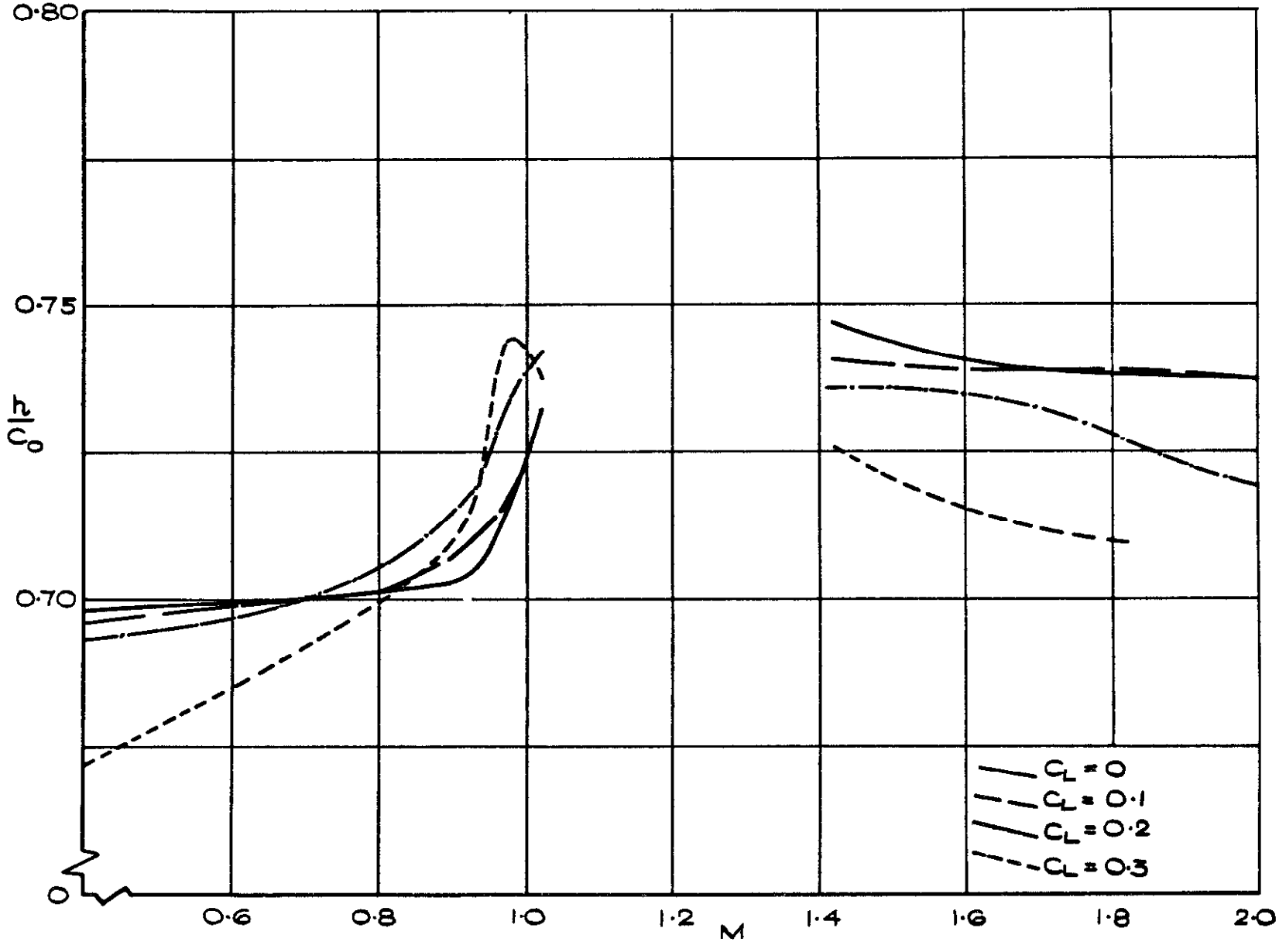

FIG.8. VARIATION OF AERODYNAMIC CENTRE POSITION WITH MACH NUMBER.

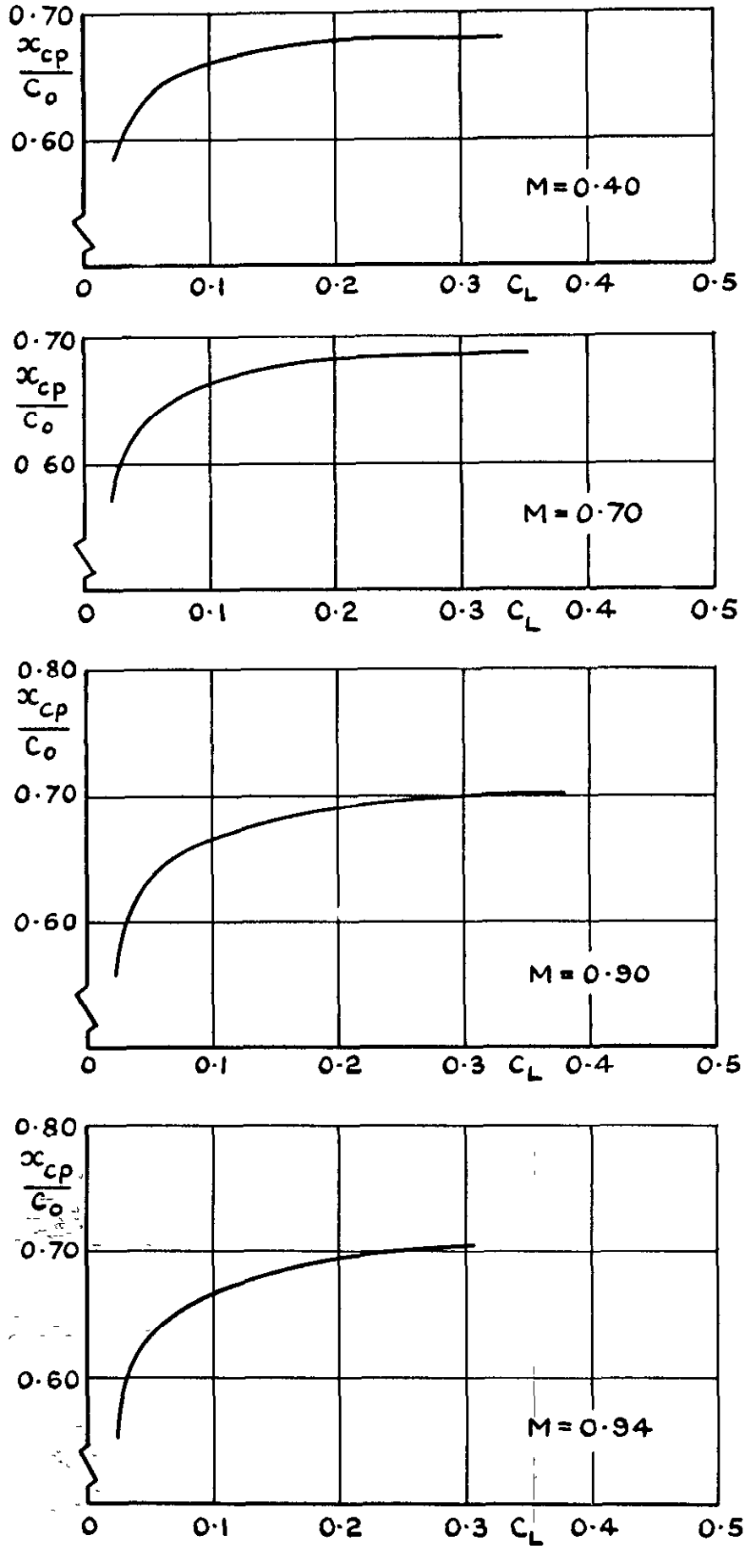

FIG. 9. VARIATION OF CENTRE OF PRESSURE POSITION WITH C_L

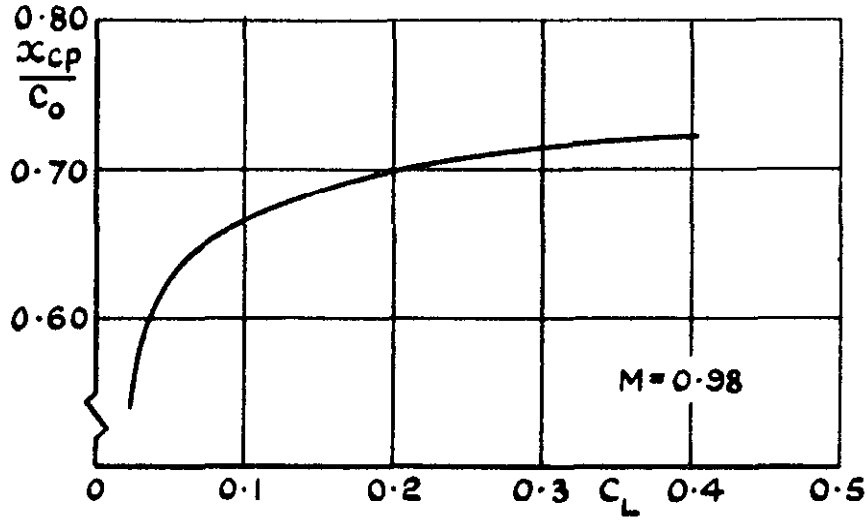
0·80
$\frac{x_{cp}}{c_o}$
0·70
0·60
M=0·98
0
0·1
0·2
0·3
C_L
0·4
0·5

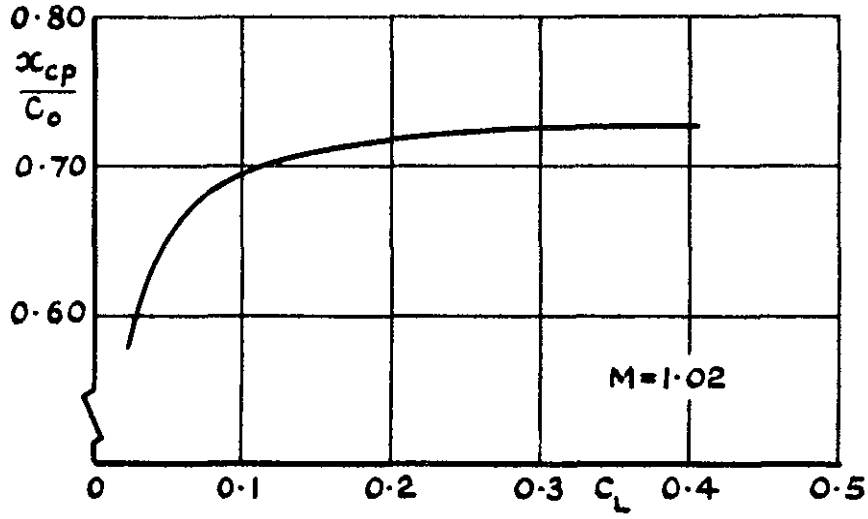
0·80
$\frac{x_{cp}}{c_o}$
0·70
0·60
M=1·02
0
0·1
0·2
0·3
C_L
0·4
0·5

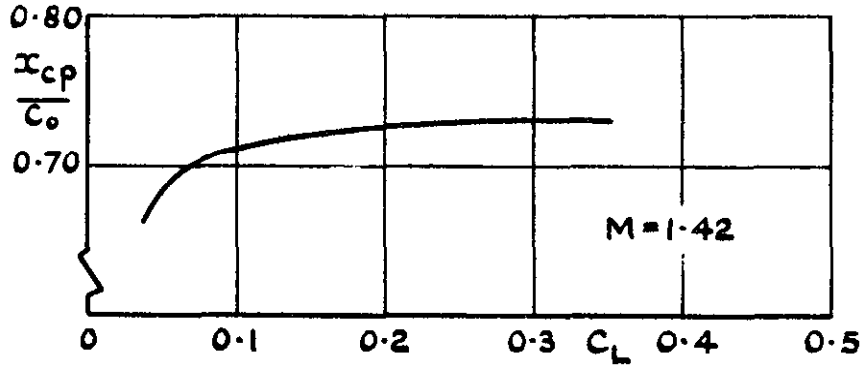
0·80
$\frac{x_{cp}}{c_o}$
0·70
M=1·42
0
0·1
0·2
0·3
C_L
0·4
0·5

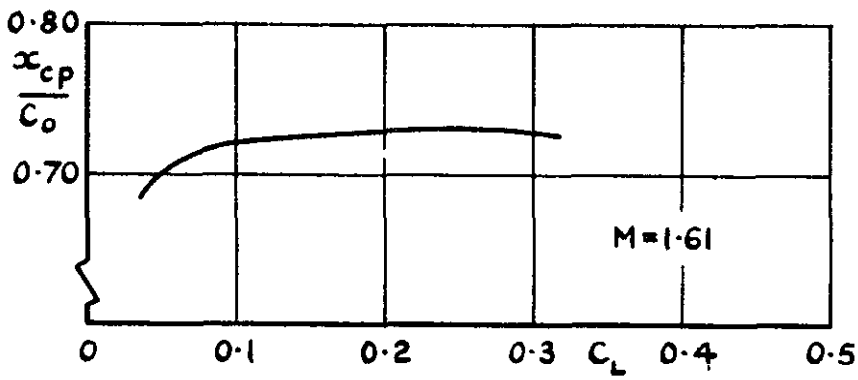
0·80
$\frac{x_{cp}}{c_o}$
0·70
M=1·61
0
0·1
0·2
0·3
C_L
0·4
0·5

FIG. 9. (CONT.)

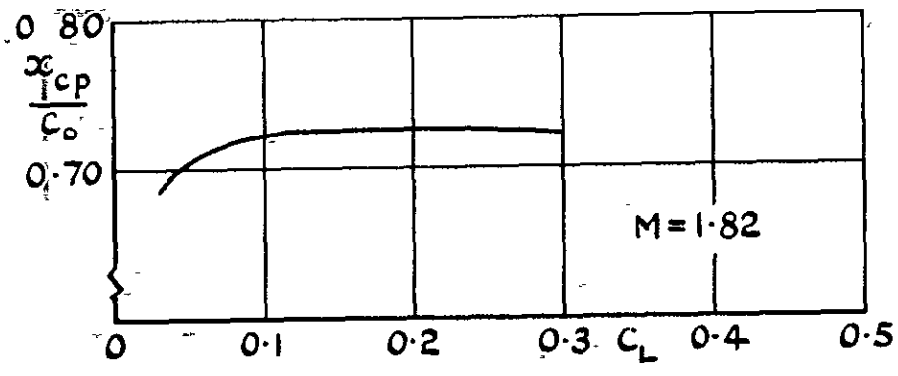
0·80
$\frac{x_{cp}}{c_o}$
0·70
M=1·82
0
0·1
0·2
0·3
C_L
0·4
0·5

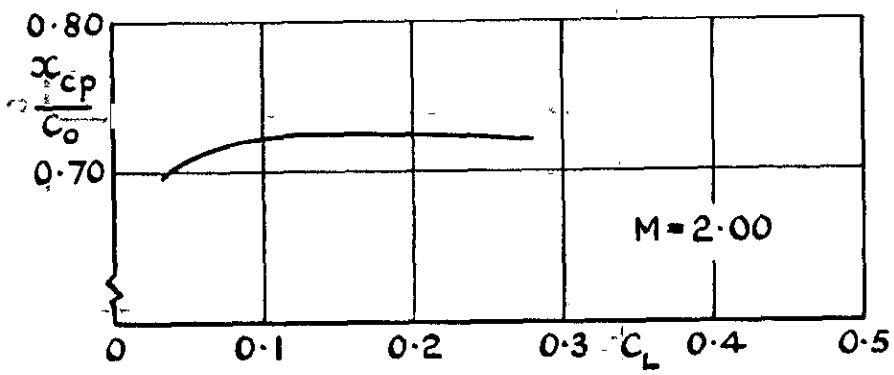
0·80
$\frac{x_{cp}}{c_o}$
0·70
M=2·00
0
0·1
0·2
0·3
C_L
0·4
0·5

FIG. 9. (CONC.)

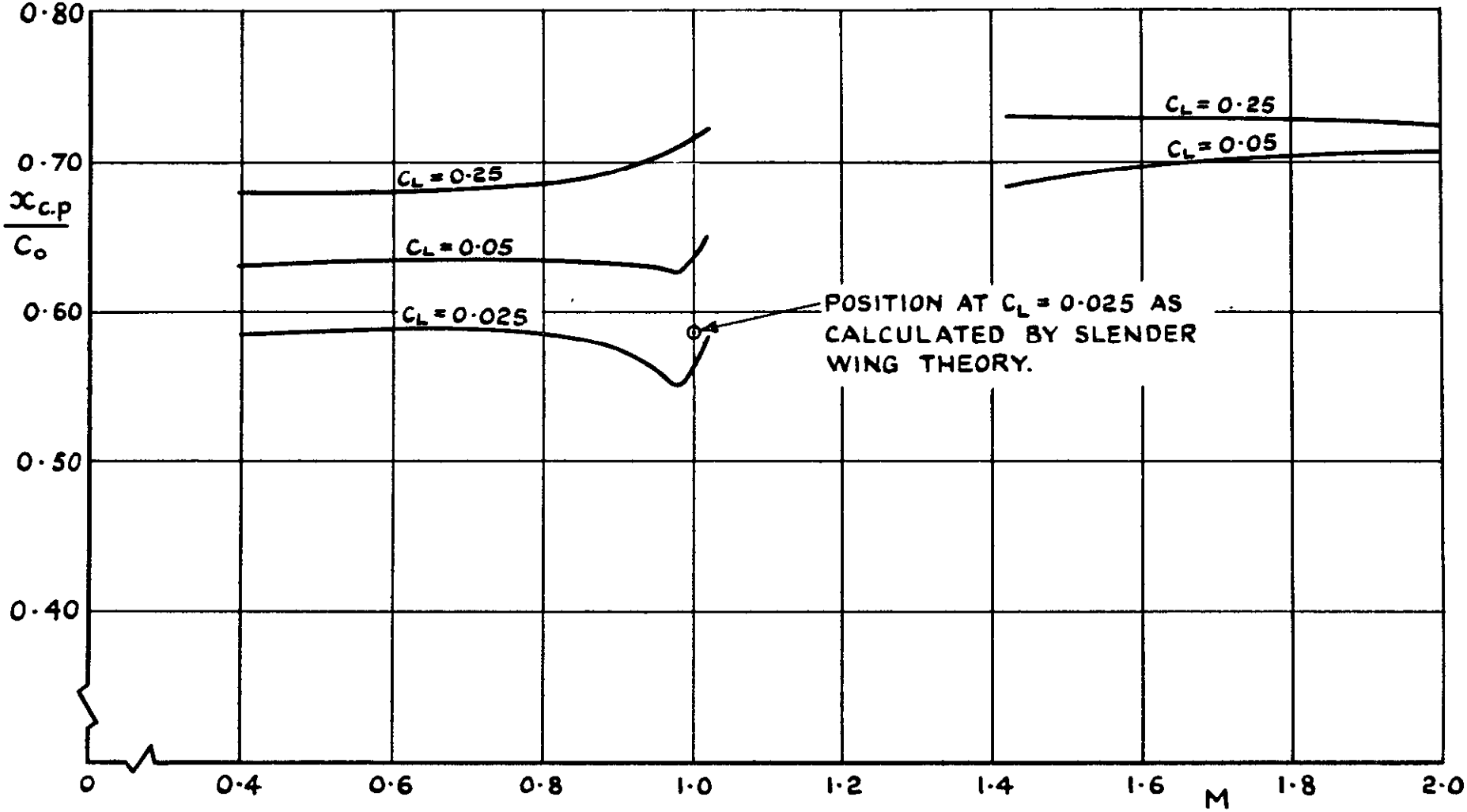

FIG. 10. VARIATION OF CENTRE OF PRESSURE POSITION WITH M FOR VARIOUS C_L VALUES.

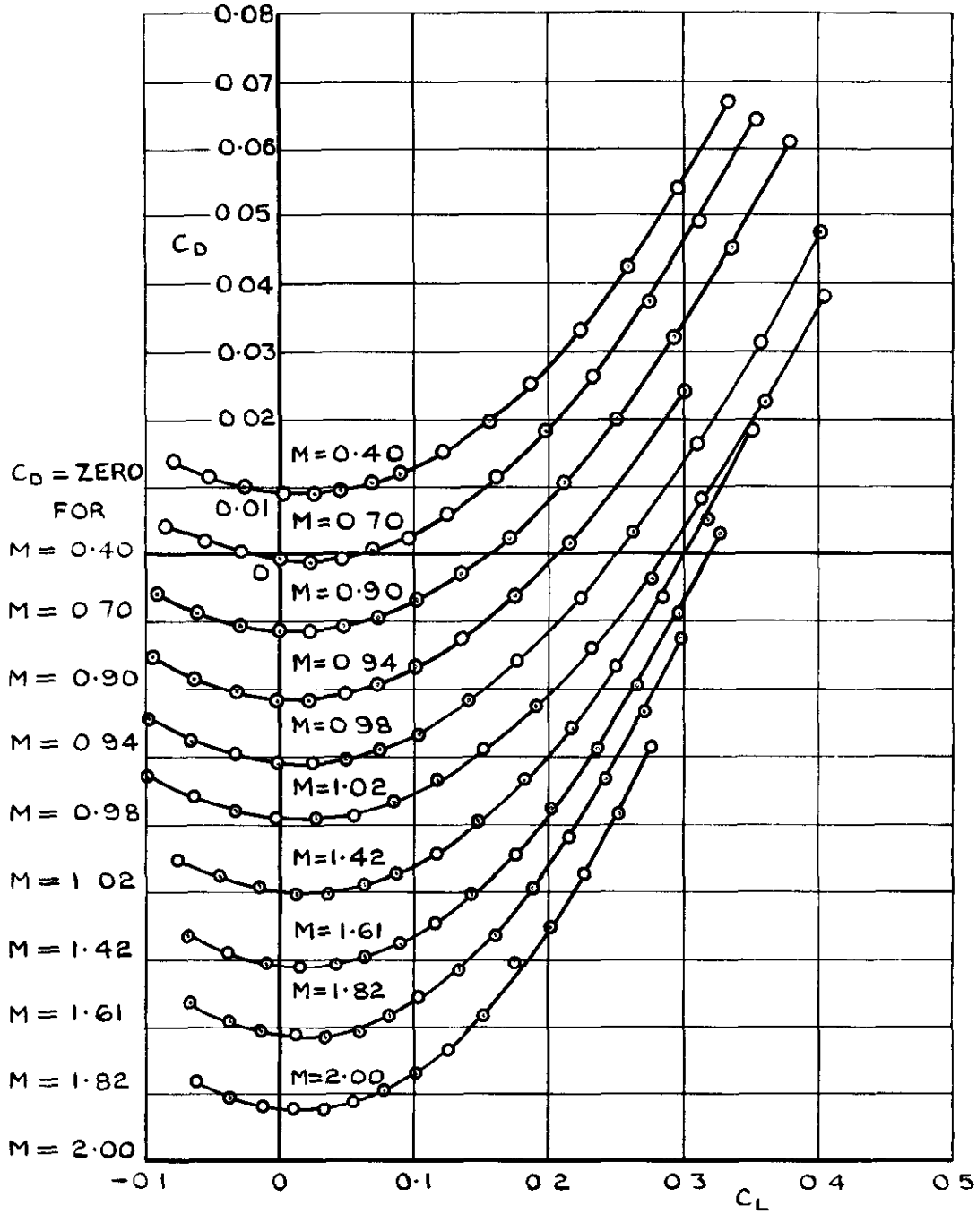

FIG. 11. VARIATION OF C_D WITH C_L

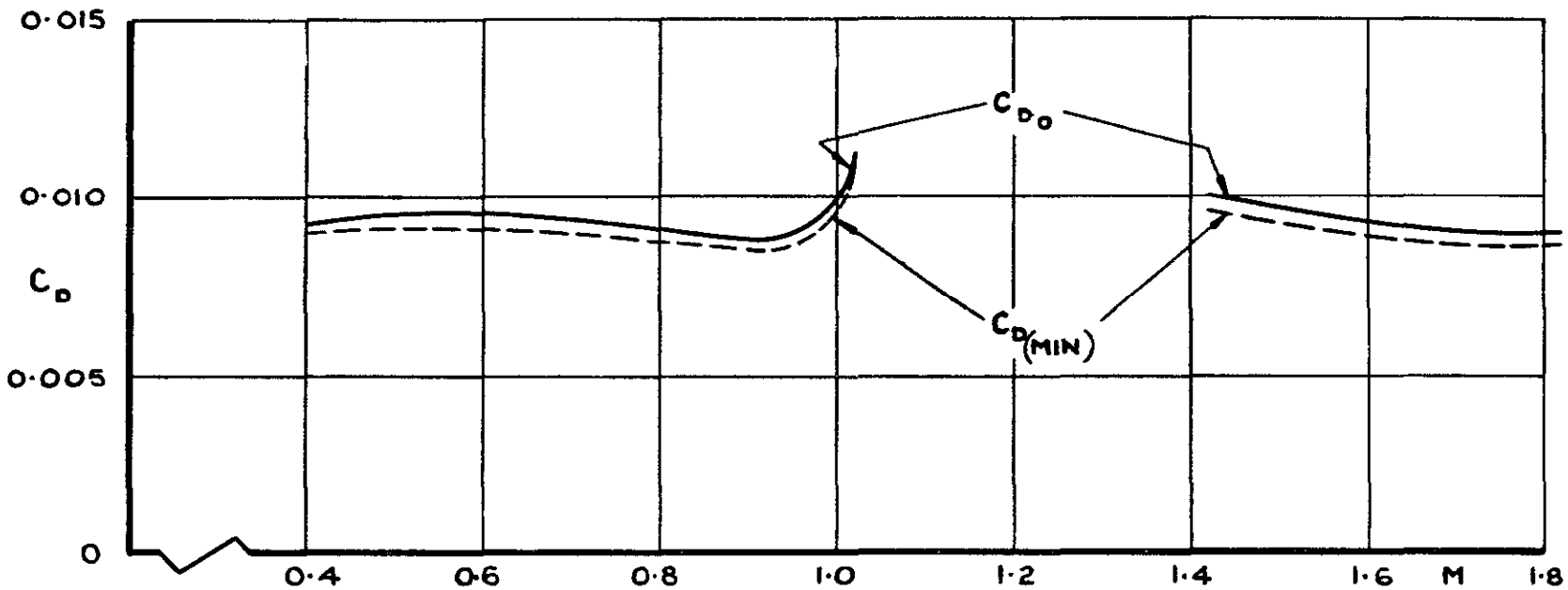

FIG. 12. VARIATION OF C_{D_0} AND $C_{D_{(MIN)}}$ WITH M.

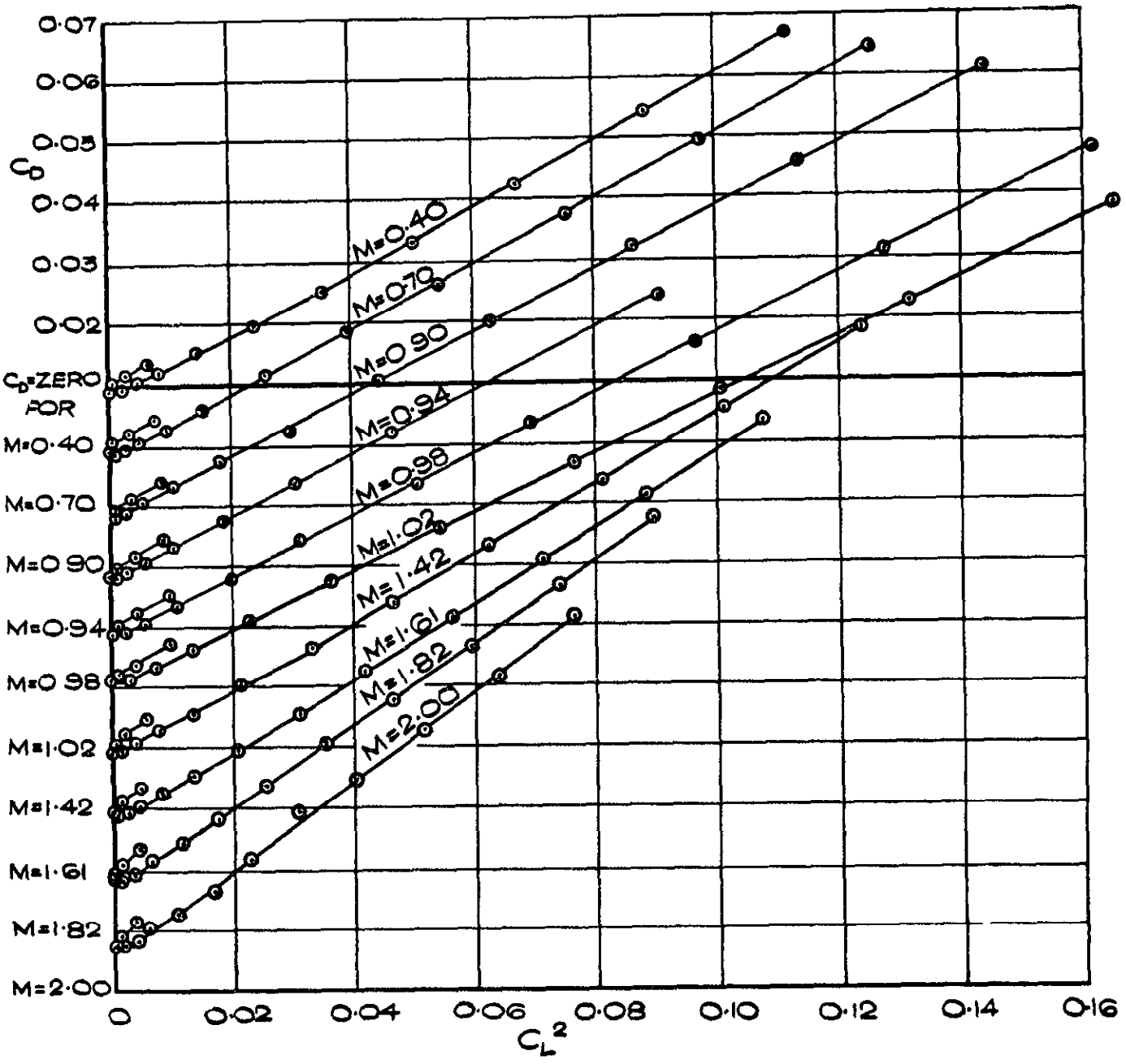

FIG. 13. VARIATION OF C_D WITH C_L^2

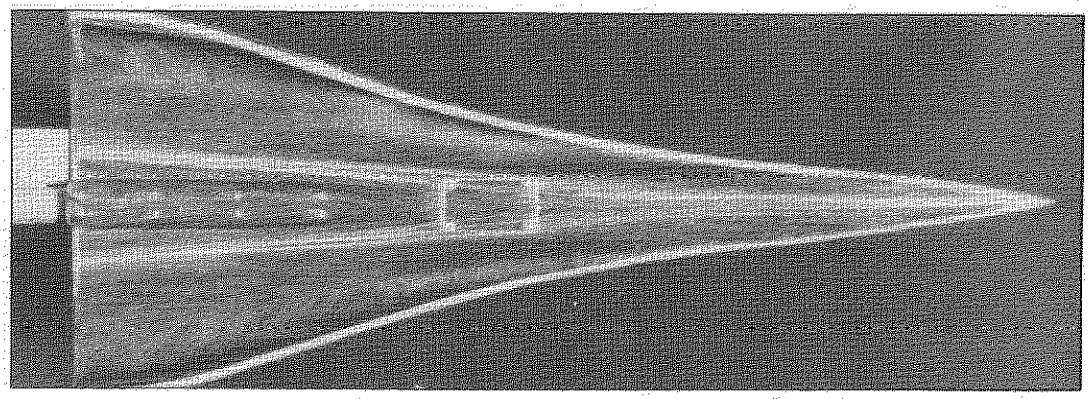

$\alpha = 7.1^{\circ}$ $C_L = 0.155$

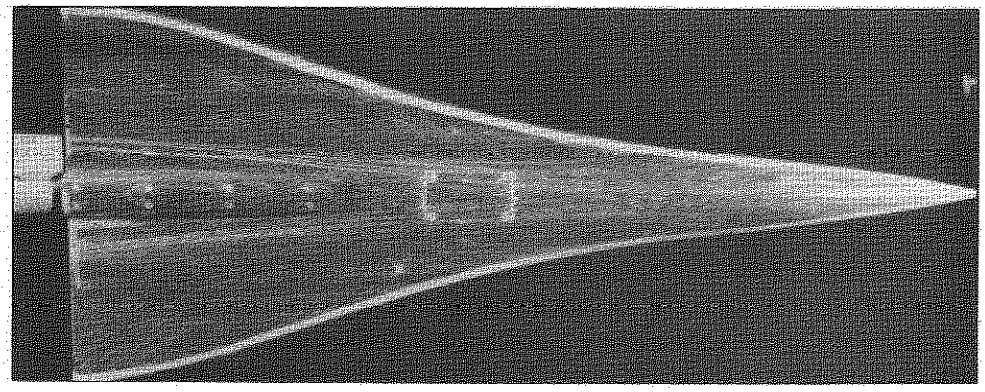

$\alpha = 6.1^{\circ}$ $C_L = 0.121$

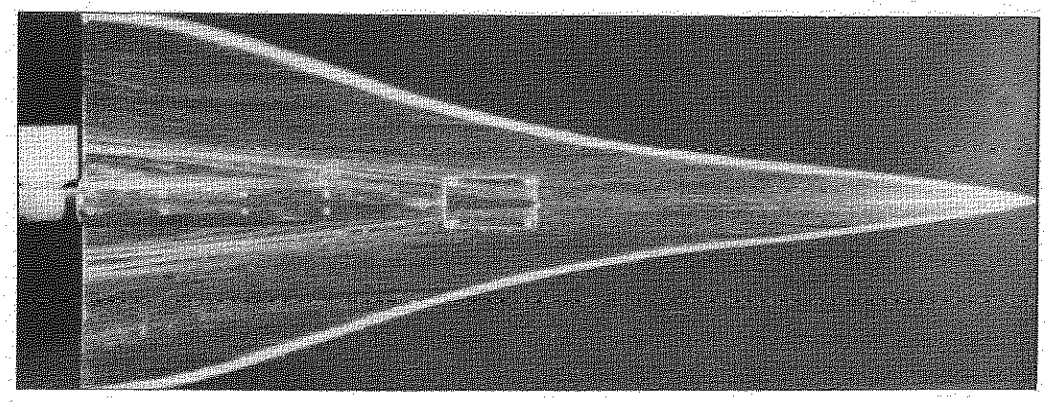

$\alpha = 5.1^{\circ}$ $C_L = 0.090$

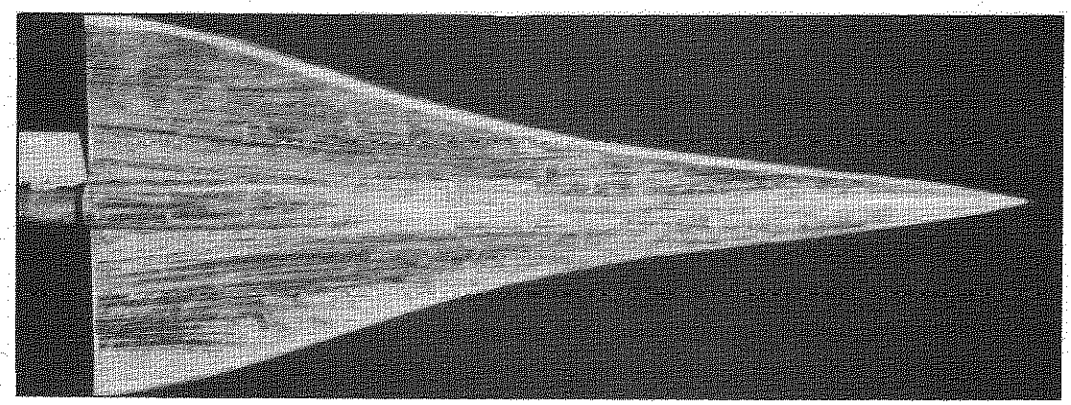

$\alpha = 4.1^{\circ}$ $C_L = 0.071$

FIG.14. FLOW PATTERNS, M = 0·40

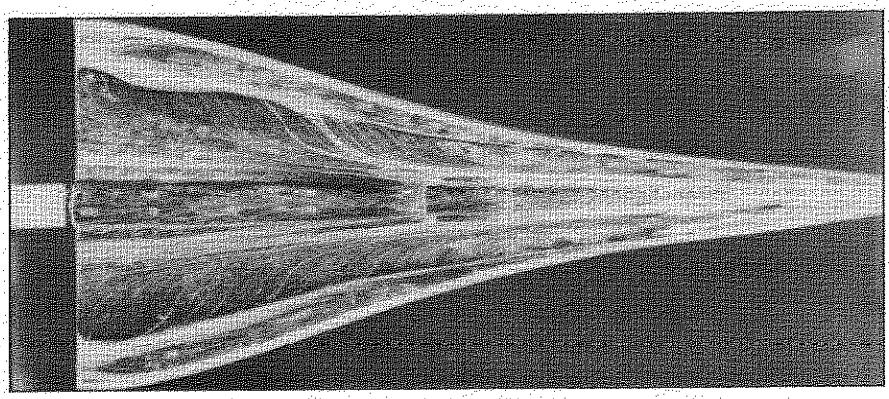

$\alpha = 10.8^{\circ}$ $C_L = 0.295$

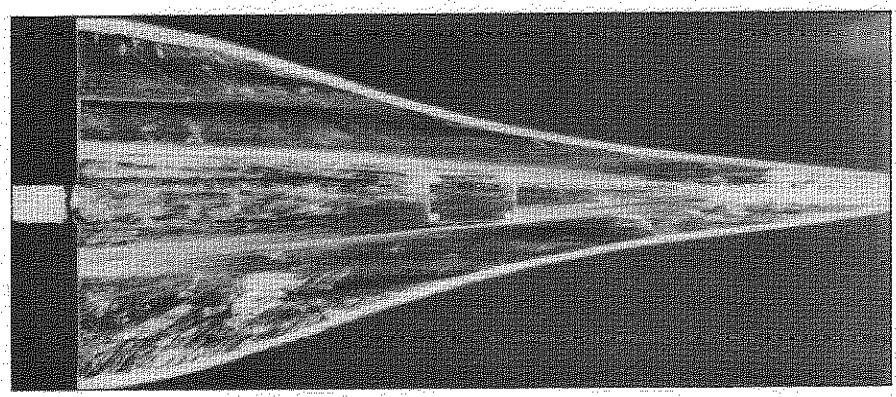

$\alpha = 6.8^{\circ}$ $C_L = 0.168$

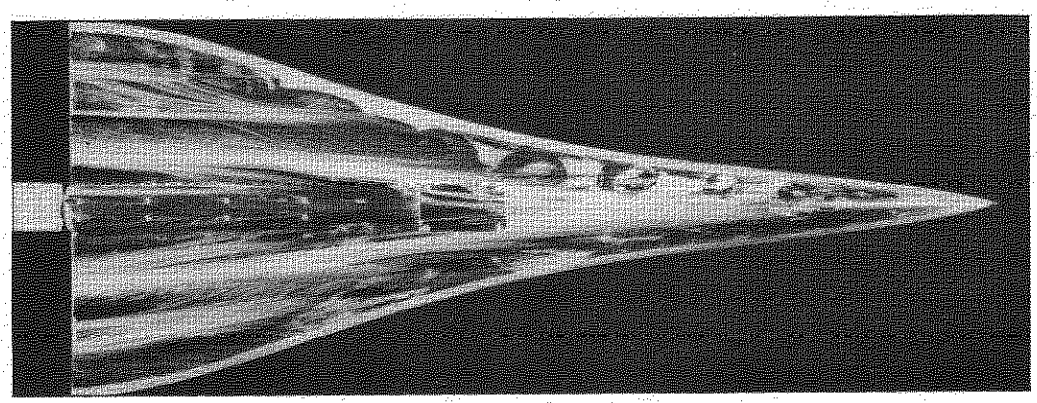

$\alpha = 5.8^{\circ}$ $C_L = 0.137$

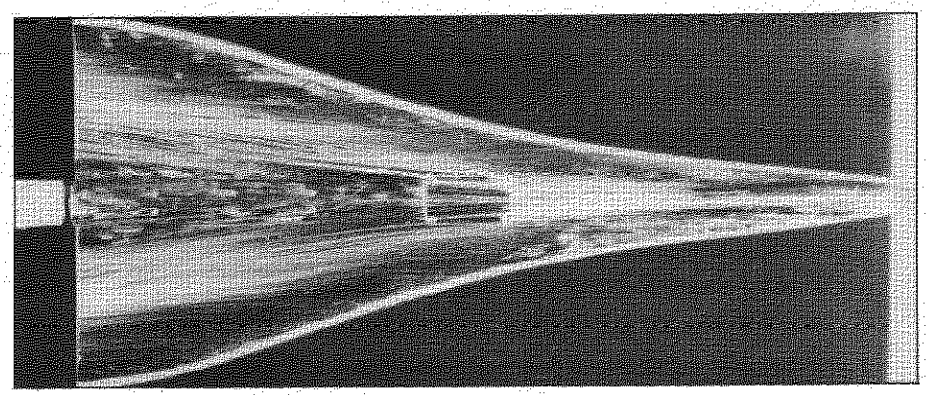

$\alpha = 4.8^{\circ}$ $C_L = 0.108$

FIG.15. FLOW PATTERNS, M = 1·42

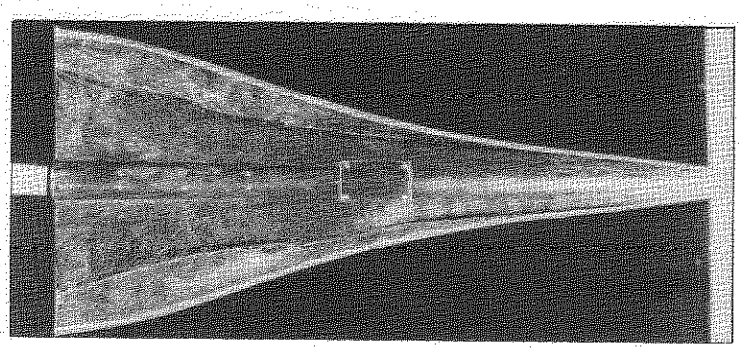

$\alpha = 10.8^{\circ}$ $C_L = 0.239$ ROUGHNESS A

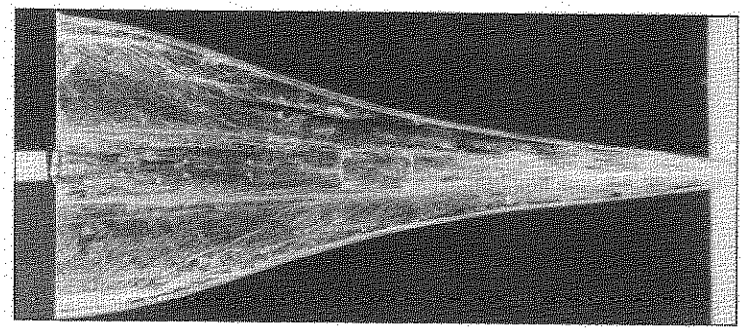

$\alpha = 8.8^{\circ}$ $C_L = 0.190$ ROUGHNESS A

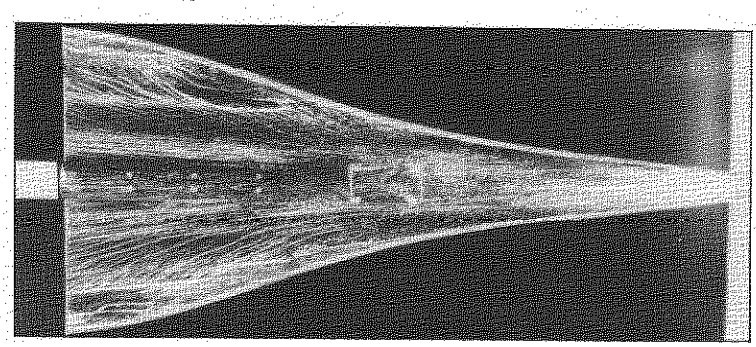

$\alpha = 6.8^{\circ}$ $C_L = 0.144$ ROUGHNESS A

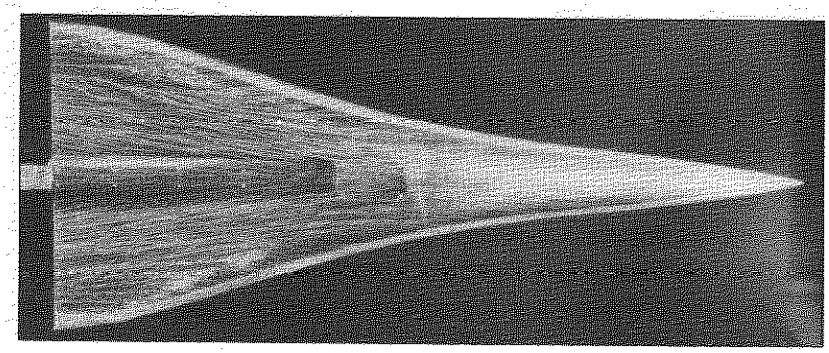

$\alpha = 4.8^{\circ}$ $C_L = 0.095$ ROUGHNESS B

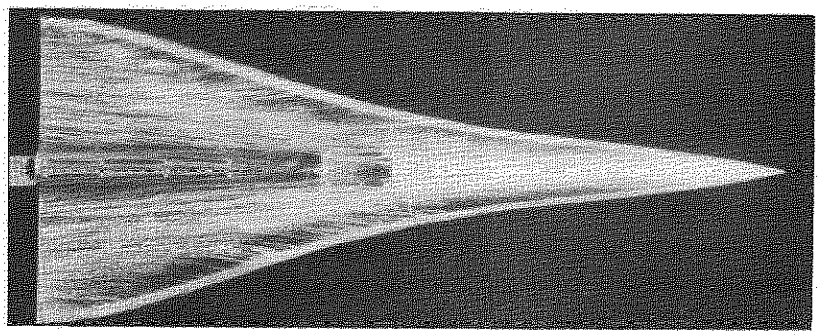

$\alpha = 2.8^{\circ}$ $C_L = 0.050$ ROUGHNESS B

FIG.16. FLOW PATTERNS, M = 2·00

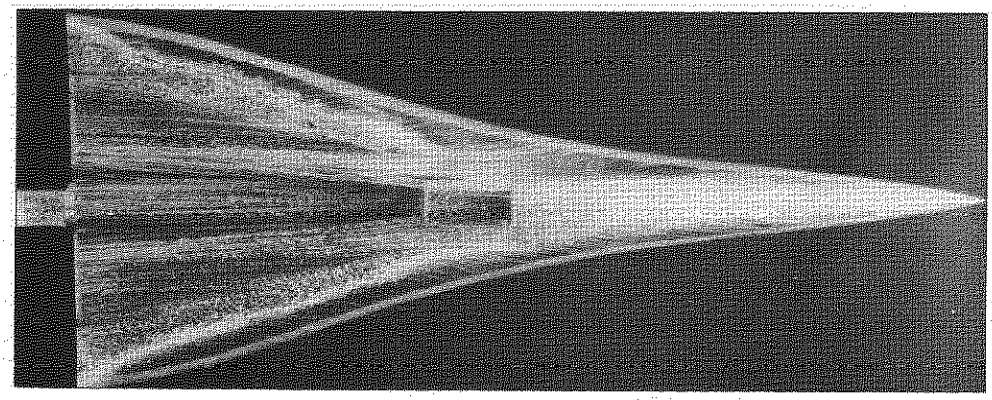

ROUGHNESS A

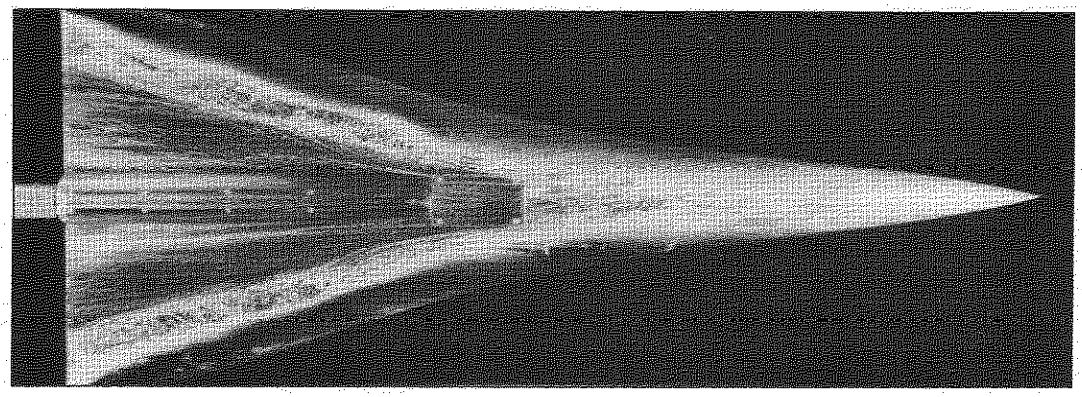

NO ROUGHNESS

FIG.17. FLOW PATTERNS, $M = 2{\cdot}00$, $\alpha = 2{\cdot}8°$, $C_L = 0{\cdot}050$.
TRANSITION NOT FIXED AT WING LEADING EDGE

A.R.C. C.P. No. 778

533.693.4 :
533.6.043.1

WIND TUNNEL TESTS BETWEEN M = 0.4 AND 2.0 ON A CAMBERED WING OF SLENDER OGEE PLANFORM.
Dobson, M.D., and King-Underwood, R. December 1963.

Results are presented of wind tunnel tests made to examine the lift, longitudinal stability and drag of a cambered wing with an ogee planform in the Mach number range 0.40 to 2.00. Some flow visualisation tests have also been made and photographs of the patterns obtained are included.

A.R.C. C.P. No. 778

533.693.4 :
533.6.043.1

WIND TUNNEL TESTS BETWEEN M = 0.4 AND 2.0 ON A CAMBERED WING OF SLENDER OGEE PLANFORM.
Dobson, M.D., and King-Underwood, R. December 1963

Results are presented of wind tunnel tests made to examine the lift, longitudinal stability and drag of a cambered wing with an ogee planform in the Mach number range 0.40 to 2.00. Some flow visualisation tests have also been made and photographs of the patterns obtained are included.

A.R.C. C.P. No. 778

533.693.4 :
533.6.043.1

WIND TUNNEL TESTS BETWEEN M = 0.4 AND 2.0 ON A CAMBERED WING OF SLENDER OGEE PLANFORM.
Dobson, M.D., and King-Underwood, R. December 1963.

Results are presented of wind tunnel tests made to examine the lift, longitudinal stability and drag of a cambered wing with an ogee planform in the Mach number range 0.40 to 2.00. Some flow visualisation tests have also been made and photographs of the patterns obtained are included.

Published by
HER MAJESTY'S STATIONERY OFFICE

To be purchased from
York House, Kingsway, London W.C.2
423 Oxford Street, London W.1
13A Castle Street, Edinburgh 2
109 St. Mary Street, Cardiff
39 King Street, Manchester 2
50 Fairfax Street, Bristol 1
35 Smallbrook, Ringway, Birmingham 5
80 Chichester Street, Belfast 1
or through any bookseller

S.O. CODE No. 23-9015-78